Enhanced spectroscopic gas sensors using in-situ grown carbon nanotubes

A. De Luca, M. T. Cole, R. H. Hopper, S. Boual, J. H. Warner, A. R. Robertson, S. Z. Ali, F. Udrea, J. W. Gardner , and W. I. Milne

Articles you may be interested in

Effect of oxygen plasma on field emission characteristics of single-wall carbon nanotubes grown by plasma enhanced chemical vapour deposition system
J. Appl. Phys. **115**, 084308 (2014); 10.1063/1.4866995

Micro-reactors for characterization of nanostructure-based sensors
Rev. Sci. Instrum. **83**, 055104 (2012); 10.1063/1.4709495

Millimeter wave carbon nanotube gas sensor
J. Appl. Phys. **101**, 106103 (2007); 10.1063/1.2734873

NO 2 and CO gas adsorption on carbon nanotubes: Experiment and theory
J. Chem. Phys. **119**, 10904 (2003); 10.1063/1.1619948

Investigation of the NO 2 sensitivity properties of multiwalled carbon nanotubes prepared by plasma enhanced chemical vapor deposition
J. Vac. Sci. Technol. B **21**, 1996 (2003); 10.1116/1.1599858

Enhanced spectroscopic gas sensors using *in-situ* grown carbon nanotubes

A. De Luca,[1] M. T. Cole,[1] R. H. Hopper,[2] S. Boual,[2] J. H. Warner,[3] A. R. Robertson,[3] S. Z. Ali,[2] F. Udrea,[1,2] J. W. Gardner,[4] and W. I. Milne[1]

[1]*Department of Engineering, University of Cambridge, Cambridge CB3 0FA, United Kingdom*
[2]*Cambridge CMOS Sensors Ltd., Deanland House, 160 Cowley Road, Cambridge CB4 0DL, United Kingdom*
[3]*Department of Materials, University of Oxford, Oxford OX1 3PH, United Kingdom*
[4]*School of Engineering, University of Warwick, Coventry CV4 7AL, United Kingdom*

In this letter, we present a fully complementary-metal-oxide-semiconductor (CMOS) compatible microelectromechanical system thermopile infrared (IR) detector employing vertically aligned multi-walled carbon nanotubes (CNT) as an advanced nano-engineered radiation absorbing material. The detector was fabricated using a commercial silicon-on-insulator (SOI) process with tungsten metallization, comprising a silicon thermopile and a tungsten resistive micro-heater, both embedded within a dielectric membrane formed by a deep-reactive ion etch following CMOS processing. *In-situ* CNT growth on the device was achieved by direct thermal chemical vapour deposition using the integrated micro-heater as a micro-reactor. The growth of the CNT absorption layer was verified through scanning electron microscopy, transmission electron microscopy, and Raman spectroscopy. The functional effects of the nanostructured ad-layer were assessed by comparing CNT-coated thermopiles to uncoated thermopiles. Fourier transform IR spectroscopy showed that the radiation absorbing properties of the CNT adlayer significantly enhanced the absorptivity, compared with the uncoated thermopile, across the IR spectrum (3 μm–15.5 μm). This led to a four-fold amplification of the detected infrared signal (4.26 μm) in a CO_2 non-dispersive-IR gas sensor system. The presence of the CNT layer was shown not to degrade the robustness of the uncoated devices, whilst the 50% modulation depth of the detector was only marginally reduced by 1.5 Hz. Moreover, we find that the 50% normalized absorption angular profile is subsequently more collimated by 8°. Our results demonstrate the viability of a CNT-based SOI CMOS IR sensor for low cost air quality monitoring. © 2015 AIP Publishing LLC. [http://dx.doi.org/10.1063/1.4921170]

In the past two decades, the development of increasingly miniaturized infra red (IR) detectors has been predominately driven by the steady growth within the IR sensing market. Applications ranging from automotive, medical, and industrial to navigation, security, and imaging all require IR radiation sensors for two main purposes: non-contact temperature measurement and gas concentration detection via non-dispersive-IR (NDIR) spectroscopy.[1] Two broad classes of IR sensors can be identified:[2] photon detectors and thermal detectors. Until relatively recently, cooled photon detectors commercially dominated due to their exceptional sensitivity. However, thermal detectors can operate at room temperature, thus enabling a wide range of low cost applications previously not accessible by photon detectors (nb. uncooled semiconductor diodes, such as InSb, are of growing interest but still too expensive for mass markets). In order to exploit this, much effort has been focused on the development of IR detectors based on thermal principles requiring no active cooling. These devices convert electromagnetic radiation into heat, which is then converted into an electrical signal which is subsequently processed for sensing information extraction. The nature of this thermo-electric transduction can be used to further define three thermal detector sub-categories, namely, bolometers, pyroelectric detectors, and thermopiles. The entire IR sensing market has simultaneously pushed for a reduction in the price of these devices whilst requiring improvement in their performance. The coupling between complementary-metal-oxide-semiconductor

(CMOS) technologies and micromachining fabrication techniques offers one viable and attractive route to achieve high-throughput manufacturing, in a cost efficient production process. Nevertheless, materials commonly used in CMOS foundries are often not pyroelectric and have poor IR absorption properties especially for wavelengths < 8 μm,[3] a spectral window of importance for NDIR gas sensing (e.g., methane and CO_2). As a consequence, bolometers and thermopiles often require at least one additional post-CMOS (and post-microelectromechanical system (MEMS)) processing step for the deposition of a radiation absorbing layer. These absorbers can be broadband[4] such as black porous metals or frequency selective[5] such as resonant structures. The best approach is typically driven by commercial, technology-compatibility, and application related considerations. In this letter, we prove, in an application with high commercial value, the effectiveness of vertically aligned multi-walled carbon nanotubes (CNTs) as blackbody-like IR absorbing layers integrated onto a CMOS-MEMS thermopile. Our approach employs an integrated micro-heater to realize *in-situ*[6] thermal chemical vapour deposition (T-CVD) growth of the CNT layer in a CMOS-compatible manner with full wafer level scalability capabilities.[7]

It has been long known how to fabricate temperature/radiation sensing devices based on the Seebeck effect,[8] which is the physical phenomenon describing the self-generation of a potential difference between the open terminals of two dissimilar materials joined together, where
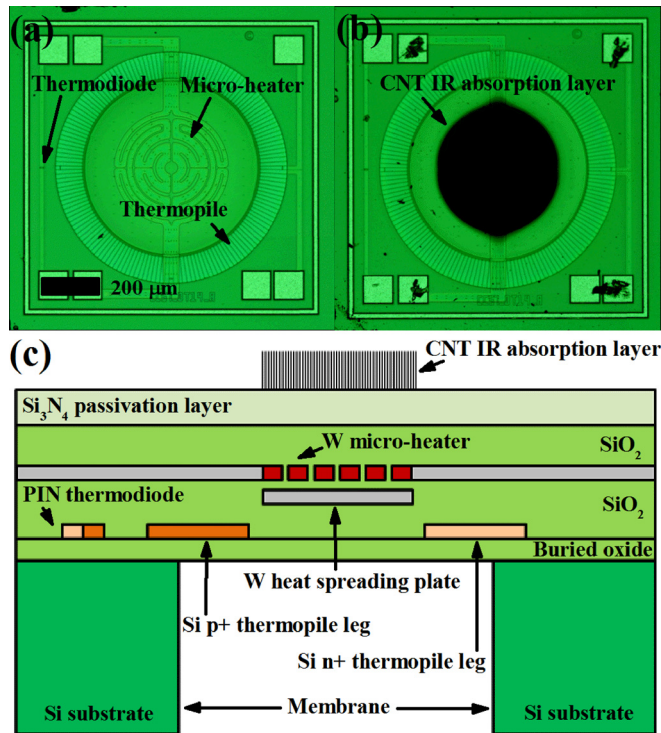
FIG. 1. (a) Optical micrograph of the IR detector chip (1.6 mm × 1.6 mm), (b) optical micrograph of the IR detector chip after CNT radiation absorbing layer *in-situ* T-CVD growth, (c) schematic cross-sectional depiction of the IR detector.

the open terminals and the junction are subject to a temperature difference. At present, thermopiles are mostly fabricated using silicon fabrication technologies, not only because semiconductors exhibit high values of the Seebeck coefficient[9] but also because they enable cost efficient production and facilitate integration with circuitry and other sensing devices on-chip. In order to obtain performance in line with the market requirements, coupling of semiconductor and micromachining techniques is essential. Semiconductor technologies open up routes towards miniaturization with the potential for on-chip system integration with IR devices. Nevertheless, micromachining is central to enabling implementation of thermal isolation schemes imperative for the reduction of thermal conduction losses which are otherwise detrimental to achieving high sensitivity and rapid response times.

In this work, we present an IR detector[10] (Fig. 1) comprising (i) a silicon $p+/n+$ thermopile, with cold junctions supported by the substrate and hot junctions embedded within a $\approx 5\,\mu m$ thick dielectric membrane (1.2 mm diameter); (ii) a tungsten microheater (600 μm diameter), for *in-situ* T-CVD growth; and (iii) a *P-I-N* diode temperature sensor, for cold junction compensation purposes. All devices were fabricated in a commercial foundry using silicon-on-insulator (SOI) CMOS technology with tungsten metallization followed by DRIE to release the membrane. The thermopile consists of 80 single crystal silicon $p+/n+$ thermocouples,
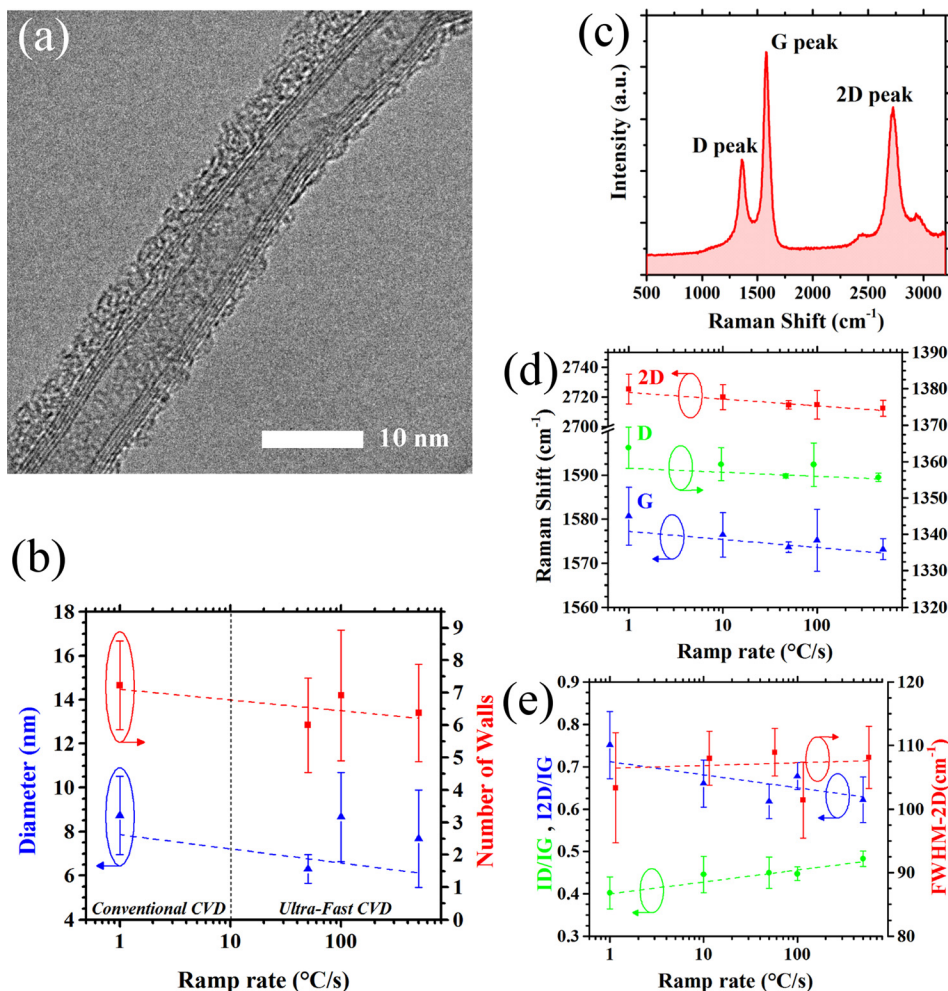

FIG. 2. (a) Typical TEM micrograph of a multi-walled CNT, (b) CNT diameter (blue) as a function of thermal ramp rate (left axis) and number of CNT graphitic side-walls (red) as a function of thermal ramp rate (right axis), (c) typical Raman spectrum of a multi-walled CNT, (d) Raman shift as a function of thermal ramp rate for G peak (blue), D peak (green), and 2D peak (red), and (e) I_D/I_G (green) and I_{2D}/I_G (blue) as a function of thermal ramp rate (left axis) and full width half maximum of 2D peak (red) as a function of thermal ramp rate (right axis).

connected via tungsten contacts to avoid the formation of *p-n* junctions. Each thermocouple leg (150 $\mu m \times 20 \mu m$) has its cold (reference) junction on the chip substrate and its hot (sensing) junction embedded within the silicon dioxide membrane along with a circular heat spreading plate (940 μm in diameter). This spreading plate reduces the equivalent thermal resistance from the centre of the membrane to the thermopile's sensing junctions and so reduces the response time of the detector. A circular multi-ring tungsten heater, designed to obtain a highly uniform temperature distribution, is integrated within the membrane, chosen to be circular to mitigate induced thermo-mechanical stresses during high temperature (700 °C) *in-situ* T-CVD processing, thereby improving the overall device robustness and yield. The diode temperature sensor,[11] embedded close to the cold junctions, provides the IR detector chip with ambient temperature compensation capabilities. A SOI substrate was chosen as the *p+/n+* silicon thermopiles are formed of the thin silicon layer in the SOI substrate. SOI also allows high ambient temperature device operation (up to 225 °C) whilst also offering an inherently high quality thermally grown buried silicon dioxide layer which acts as an effective etch stop for the post-CMOS DRIE.

The integration of the CNT radiation absorbing layer was achieved in-house by *in-situ* T-CVD. Typically, CNT growth requires temperatures in excess of 400 °C, which readily damages the CMOS circuitry and the Al pad layer. Due to their design, our micro-hotplates are capable of reaching temperatures in excess of 750 °C in an isolated localized "hot zone," without compromising the chip functionality. Such micro-heaters can be effectively employed as CMOS compatible micro-reactors and allow viable CNT-CMOS integration at chip and wafer level by parallelizing the growth on several devices simultaneously.[7] In the present study, the CNT radiation absorbing layer was grown at 25 mbar from a bilayer catalyst Al/Fe (10/1 nm) in a 4% $H_2:C_2H_2$ atmosphere at 700 °C for 10 min. The micro-reactors were controlled with a LabView integrated Keithley 2401 source meter. For accurate temperature and growth timing control, a temperature loop feedback was implemented at the software level. CNT growth was verified by optical microscopy (Fig. 1(b)), where the CNT "forest" is clearly observed on the micro-heater area.

The micro-heaters are characterized by very fast thermal transient times. Our micro-reactors can heat from room temperature to 700 °C, typically within a few tens of milliseconds, with a maximum thermal ramp rate of 10^4 °C/s. However, *in-situ* T-CVD proved to be unsuccessful under these ultra-fast thermal ramps. The sudden rise or fall of temperature, coupled with the low pressure environment required by the CVD process, resulted in catastrophic damage to the membranes. To promote optimal CNT growth, the thermal ramp rate for CNT growth was controlled (at software level) under equivalent growth conditions at thermal ramps of 1 °C/s, 50 °C/s, 100 °C/s, and 500 °C/s. It was found that the yield increased by reducing the thermal transient time, with yields approaching 100% for thermal ramps <50 °C/s. Optimal conditions were found when the thermal ramp rates were reduced to 10 °C/s; this minimized thermo-mechanical stress on the membrane thereby avoiding breakages and concurrently

maintaining the total growth time <5 min. Transmission electron microscopy (TEM) analysis (Figs. 2(a) and 2(b)) showed the tubes' diameter to be approximately 8 nm with, on average, 5–9 graphitic side-walls. Minimal dependence of the tubes' diameter and number of side-walls on the ramp rates was observed. Raman spectra (Fig. 2(c)), were also consistent with those reported in literature[12] for multi-walled CNTs and marginally affected by the thermal ramp rates (Figs. 2(d) and 2(e)).

Scanning electron microscopy (SEM) inspection confirmed the successful growth of the vertically aligned CNT based absorbing layer (Fig. 3(a)). The IR absorption properties of the coated and uncoated devices were studied via Fourier transform IR (FTIR) spectroscopy (Fig. 3(b)). Transmission (T) and reflection (R) FTIR measurements (normal incidence) were coupled in order to obtain the absorption ($A = 1 - R - T$) spectral profiles in the wavelength range of 3 μm–15.5 μm. The optical aperture of the micro-FTIR system (FTS 7000 FTIR spectrometer with UMA 600 microscope) was set to image only the heater area of the IR detectors. The *in-situ* grown absorption layer was found to have nearly unitary absorptivity, in contrast to the uncoated detectors which were characterized by an absorption peak around 8.5 μm, attributed to the Si-O stretching vibration[13] within the SiO_2 membrane, consistent with previously reported findings.[14] Even though the CNT IR absorption properties have been intensively studied,[15–19] very little work has dealt with their exploitation in commercially
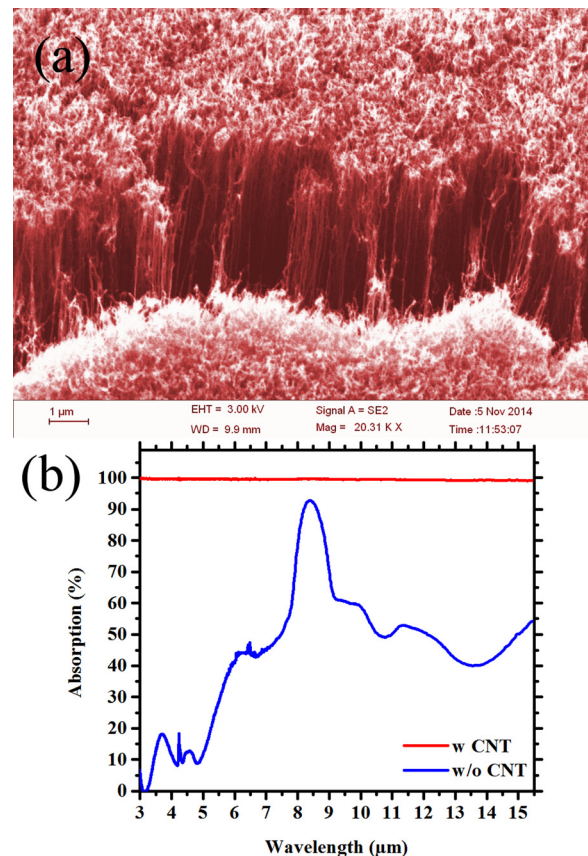

FIG. 3. (a) SEM micrograph of the CNT-based IR radiation absorbing layer and (b) comparison between FTIR spectra of CNT coated and uncoated devices.
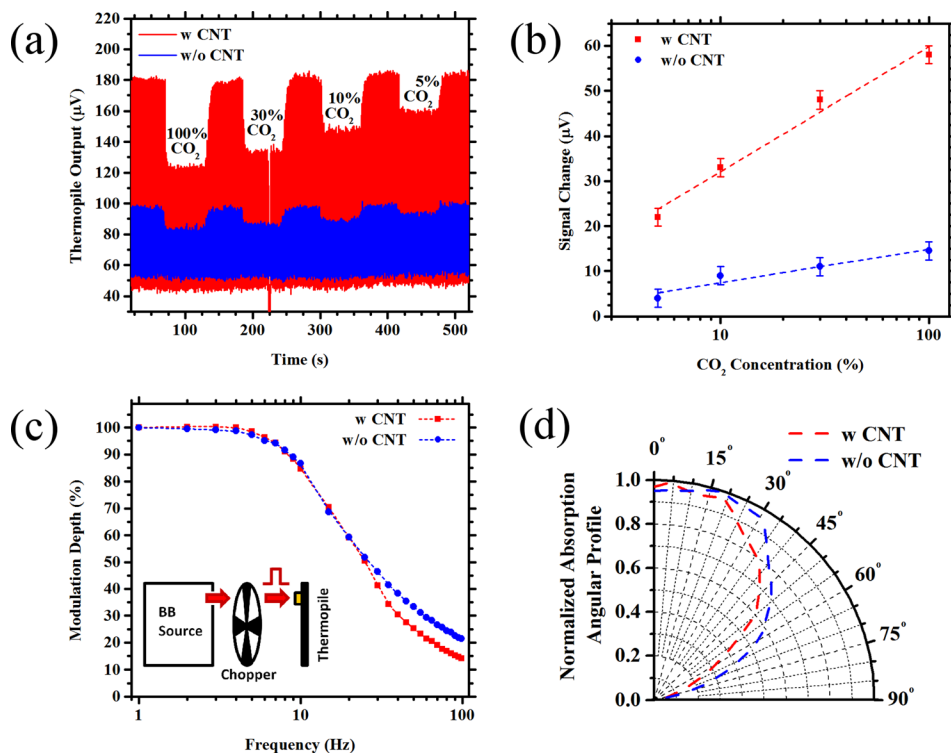
FIG. 4. (a) Raw thermopile output under IR source pulsed excitation (1 Hz, 50% duty cycle) for different CO_2 concentrations in dry air, (b) extrapolated sensitivity of NDIR sensor employing coated and uncoated thermopile, (c) modulation depth for coated and uncoated thermopile, and (d) normalized absorption angular profile for coated and uncoated thermopile.

practical applications. Lehman *et al.*[20] showed that vertically aligned multi-walled CNTs can be effectively employed for sensitivity enhancement of pyroelectric IR detectors, while we have previously shown[21,22] that CNTs can improve the thermo-optical transduction efficiency of IR thermal emitters used for NDIR spectroscopy.

In Fig. 4(a), we evaluate the performance of the CNT coated IR detectors in a capnometer-like NDIR CO_2 sensor with a path length of 7.5 mm over the 5%–100% CO_2 concentration (C_{CO2}) range. Under IR illumination, the detectors' signal drops due to CO_2 radiation absorption. The detector's signal change (SC), plotted in Fig. 4(b), is enhanced by a factor of four following the inclusion of the CNT-based ad-layer due to its intrinsic superior opto-thermal conversion efficiency. An equivalent improvement is additionally observed in the signal-to-noise ratio, since the noise floor of 2 μV is dominated by thermal noise due to the detectors internal resistance and noise associated with cabling, and in the sensitivity of the system ($S_{wCNT} = 14.2/C_{CO2}$, $S_{w/oCNT} = 3.8/C_{CO2}$), defined as dSC/dC_{CO2}. The response time of the NDIR system (< 5 s) was governed by the flow dynamics of the gas test system. The thermopiles prove to have response times of < 100 ms (Fig. 4(c)). We further studied the effect of the CNT layer on the detectors' modulation depth, an important figure of merit for NDIR pulse mode operation which is commonly used to reduce $1/f$ noise and power consumption. The CNT ad-layer was found to cause a negligible degradation of only 1.5 Hz in the 50% modulation depth. The detector angular absorption profile (Fig. 4(d)) was also improved following CNT inclusion, with the subsequent collimation of the 50% normalized absorption angular profile improving by 8°.

In order to assess device robustness, impact tests were performed from a height of 2 m on samples bonded inside cap-fitted TO39 packages. All components were not under any external physical control; the impact angle varied with each drop as did the recoil heights. Devices were optically inspected and electrically tested before and after each drop. No optical and electrical changes were observed after a set of 6 drops for multiple devices. The CNT ad-layers exhibited excellent adherence on the thermopile passivation layer proving that the extra mass of the CNT layer does not to affect the mechanical robustness of the membranes.

In conclusion, we have integrated and demonstrated the practical application of CNTs on CMOS thermopile IR detectors to realize a nano-engineered radiation absorbing layer via the use of *in-situ* T-CVD. We have extensively characterized the CNT layer by optical microscopy, SEM, TEM, Raman and FTIR spectroscopy, showing a significant enhancement (+370%) in the absorption properties of coated thermopiles relative to their uncoated counterpart. Application of the IR detector in CO_2 NDIR spectroscopic gas sensor was also demonstrated, resulting in a sensitivity enhancement of four times, opening up unprecedented possibilities for nano-materials exploitation in the IR micro-sensor market.

[1]J. Hodgkinson, R. Smith, W. O. Ho, J. R. Saffell, and R. P. Tatam, Sens. Actuators, B **186**, 580 (2013).
[2]A. Rogalski, Prog. Quantum Electron. **27**(2), 59 (2003).
[3]A. De Luca, M. T. Cole, A. Fasoli, S. Z. Ali, F. Udrea, and W. I. Milne, J. Appl. Phys. **113**(21), 214907 (2013).
[4]W. Lang, K. Kühl, and H. Sandmaier, Sens. Actuators, A **34**(3), 243 (1992).
[5]J. J. Talghader, A. S. Gawarikar, and R. P. Shea, Light: Sci. Appl. **1**(8), e24 (2012).
[6]M. S. Haque, K. B. K. Teo, N. L. Rupensinghe, S. Z. Ali, I. Haneef, S. Maeng, J. Park, F. Udrea, and W. I. Milne, Nanotechnology **19**(2), 025607 (2008).

[7]S. Santra, S. Z. Ali, P. K. Guha, G. Zhong, J. Robertson, J. A. Covington, W. I. Milne, J. W. Gardner, and F. Udrea, Nanotechnology **21**(48), 485301 (2010).

[8]A. Graf, M. Arndt, M. Sauer, and G. Gerlach, Meas. Sci. Technol. **18**(7), R59 (2007).

[9]S. C. Allison, R. L. Smith, D. W. Howard, C. Gonzalez, and S. D. Collins, Sens. Actuators, A **104**(1), 32 (2003).

[10]F. Udrea, J. W. Gardner, S. Z. Ali, M. F. Chowdhury, and I. Poenaru, U.S. patent 8,552,380 (8 October 2013).

[11]A. De Luca, V. Pathirana, S. Z. Ali, D. Dragomirescu, and F. Udrea, Sens. Actuators, A **222**, 31 (2015).

[12]L. Bokobza and J. Zhang, Express Polym. Lett. **6**(7), 601 (2012).

[13]D. A. Kumar, J. M. Shyla, and F. P. Xavier, Appl. Nanosci. **2**(4), 429 (2012).

[14]K. Mizuno, J. Ishii, H. Kishida, Y. Hayamizu, S. Yasuda, D. N. Futaba, M. Yumura, and K. Hata, Proc. Natl. Acad. Sci. U.S.A. **106**, 6044 (2009).

[15]F. J. Garcia-Vidal, J. M. Pitarke, and J. B. Pendry, Phys. Rev. Lett. **78**(22), 4289 (1997).

[16]Z.-P. Yang, L. Ci, J. A. Bur, S.-Y. Lin, and P. M. Ajayan, Nano Lett. **8**(2), 446 (2008).

[17]M. Wąsik, J. Judek, M. Zdrojek, and A. M. Witowski, Mater. Lett. **137**, 85 (2014).

[18]S. Mukherjee and A. Misra, J. Phys. D: Appl. Phys. **47**(23), 235501 (2014).

[19]N. A. Tomlin, A. E. Curtin, M. White, and J. H. Lehman, Carbon **74**, 329 (2014).

[20]J. Lehman, A. Sanders, L. Hanssen, B. Wilthan, J. Zeng, and C. Jensen, Nano Lett. **10**(9), 3261 (2010).

[21]A. De Luca, M. T. Cole, R. H. Hopper, S. Z. Ali, F. Udrea, J. W. Gardner, and W. I. Milne, Procedia Eng. **87**, 839 (2014).

[22]A. De Luca, Z. Racz, M. T. Cole, S. Z. Ali, F. Udrea, J. W. Gardner, and W. I. Milne, in *IEEE* Sensors (2013), p. 1.